Polymer Testing 106 (2022) 107459

Contents lists available at ScienceDirect

Polymer Testing

journal homepage: www.elsevier.com/locate/polytest

# Dielectric and ionic transport properties of bio-based polyurethane acrylate solid polymer electrolyte for application in electrochemical devices

Tuan Syarifah Rossyidah Tuan Naiwi [a], Min Min Aung [b,c,*], Marwah Rayung [b], Azizan Ahmad [d], Kai Ling Chai [b], Mark Lee Wun Fui [e,g], Emma Ziezie Mohd Tarmizi [f,h], Nor Azah Abdul Aziz [f,h]

[a] Department of Chemistry, Faculty of Science, Universiti Putra Malaysia, 43400, UPM Serdang, Selangor, Malaysia
[b] Higher Education Centre of Excellence (HiCoE), Institute of Tropical Forestry and Forest Products, University Putra Malaysia, 43400, UPM Serdang, Selangor, Malaysia
[c] Chemistry Division, Centre of Foundation Studies for Agricultural Science, University Putra Malaysia, 43400, UPM Serdang, Selangor, Malaysia
[d] School of Chemical Science and Food Technology, Faculti of Science and Technology, Universiti Kebangsaan Malaysia, 43600, Bangi, Selangor, Malaysia
[e] Department of Chemistry, Faculty of Science, University Teknologi Malaysia, 81310, UTM, Johor Bahru, Malaysia
[f] Physics Division, Centre of Foundation Studies for Agricultural Science, Universiti Putra Malaysia, 43400, UPM Serdang, Selangor, Malaysia
[g] Research Center for Quantum Engineering Design, Department of Physics, Faculty of Science and Technology, Universitas Airlangga, Jl. Mulyorejo, Surabaya, 60115, Indonesia
[h] Department of Physic, Faculty of Science, Universiti Putra Malaysia, 43400, UPM Serdang, Selangor, Malaysia

ARTICLE INFO

*Keywords:*
Biopolymer electrolyte
Jatropha oil
Lithium perchlorate
Polyurethane acrylate
Conductivity
UV radiation

ABSTRACT

Solid polymer electrolyte has been extensively studied as an alternative to liquid electrolyte that is often affected by the leakage, deformation and limited range of operating temperature issues. The present study was conducted in an attempt to synthesize polyurethane acrylate (PUA) as a host polymer to evaluate polymer performance supplemented with Li salt as polymer electrolytes. PUA was prepared by the reaction of jatropha oil polyol with toluene 2,4-diisocyanate and hydroxylethylmethylacrylate. Lithium perchlorate ($LiClO_4$) salt with different percentage of weight in the range of 5 wt. % to 25 wt. % was added to PUA to produce the PUA electrolyte. The mixtures were cured under UV radiation to obtain thin polymeric films with good thermal stability and ionic conductivity. PUA with 25 wt. % lithium salt has the highest conductivity of $6.40 \times 10^{-5}$ S $cm^{-1}$ at room temperature. The finding was supported by Fourier transform infrared (FTIR). Electrode polarization occurrence was interpreted by the complex dielectric constant ($\mathcal{E}_r$), dielectric loss ($\mathcal{E}_i$), real electrical modulus ($M_r$), imaginary electrical modulus ($M_i$) and tan σ. The effect of lithium salt addition was investigated by differential scanning calorimeter (DSC), thermogravimetric analysis (TGA), X-ray diffraction (XRD) and scanning electron microscopy (SEM) analyses. Additionally, the ionic transport properties, transference number measurement and electrochemical stability were presented.

## 1. Introduction

The SPE is well known for its lightweight property coupled with their dynamic shape conformity and improved safety profile [1]. A potential SPE of interest encompasses the use of polyurethane (PU). PU possesses good mechanical properties, low toxicity and fire resistance. PU has good water and solvent resistance as a result from its specific segmented structure and complements polymeric features of SPE [2]. Polyurethane acrylate (PUA) is a derivative of PU and it possesses oxyethylene chains in the host polymer matrices that are capable to yield higher ionic conductivity at elevated temperatures. The improvement on the mechanical properties and dimensional stability of polyurethane polymer is imperative to obtain better conductivity at ambient temperature. Besides, the higher segmental motion of polyether soft segments and low glass transition temperature, $T_g$ leads to a higher mobility of the dissolved ion which translates to a higher conductivity of the polymer electrolyte at ambient temperature [3,4]. The existence of the hard and soft segments of the PUA provides better compatibility with the addition of lithium salt for enhance conductivity, therefore suitable for use as a SPE [5,6].

The earlier study on SPE used petrochemical derived polymer such as polyethylene oxide [7], polyvinyl chloride [8], polyvinyl alcohol [9]

* Corresponding author. Higher Education Centre of Excellence (HiCoE), Institute of Tropical Forestry and Forest Products, University Putra Malaysia, 43400, UPM Serdang, Selangor, Malaysia.
*E-mail address:* minmin_aung@upm.edu.my (M.M. Aung).

https://doi.org/10.1016/j.polymertesting.2021.107459
Received 10 August 2021; Received in revised form 8 December 2021; Accepted 24 December 2021
Available online 4 January 2022

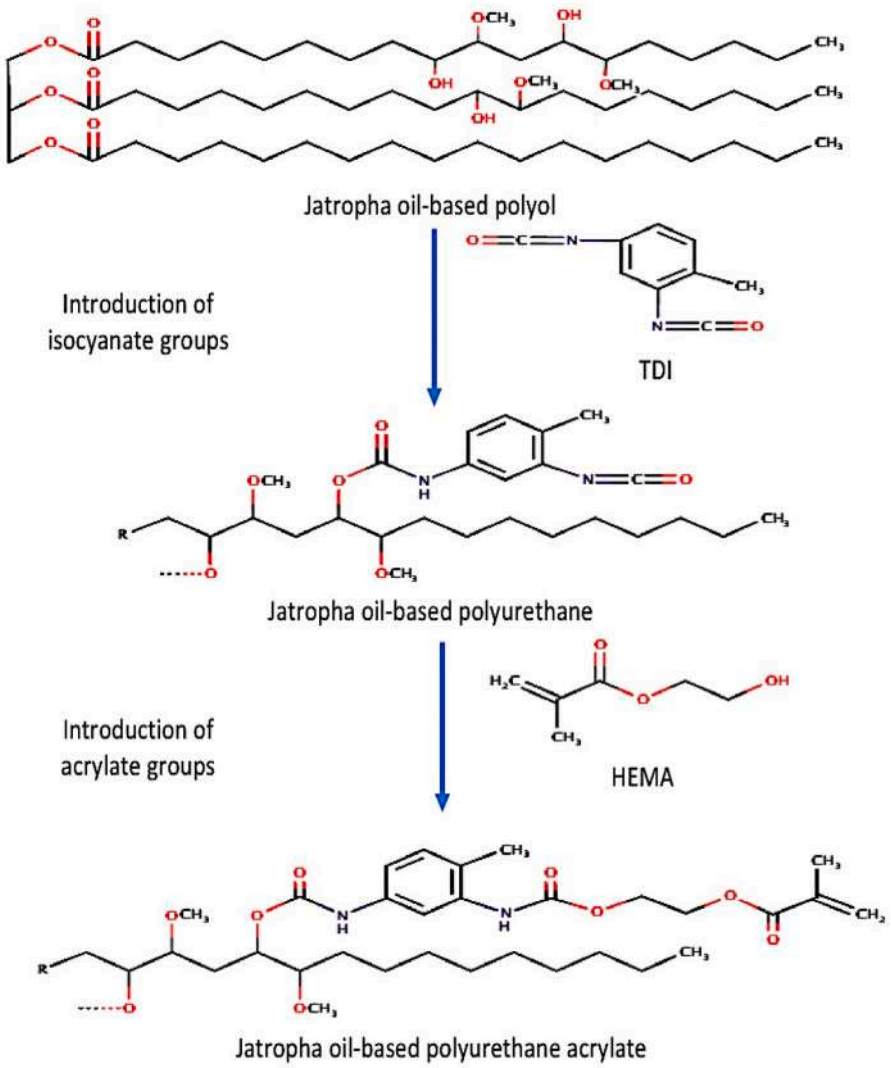


**Fig. 1.** Production of jatropha oil-based PUA.

and others as host polymer. A recent study is more oriented on developing bio-based polymers because of the environmental issues, frequent fluctuation of petroleum price and its non-renewable resources. These polymers possess advantages such as environmentally friendly, low-cost, abundance and sustainable. In general, bio-based polymer is defined as the polymer that can be obtained naturally, whether derived from plants, trees, bacteria, algae or other bio-renewable resources [10]. There are two types of the bio-based polymer which is biopolymer obtained directly from natural resources such as cellulose, protein, starches and polyester, and bio-based polymer synthesized from bio-based monomer. In the SPE field, various types of biopolymer have been investigated such as starch [11], cellulose [12], carrageenan [13], chitosan [14,15] and more. Bio-based polymer derived from vegetable oil has attracted attention to be served as polymer electrolyte. Vegetable oils have been established as singular, largest, non-toxic, non-polluting, biodegradable material yielding resins that can compete with fossil fuel-derived petro-based products. Previous studies on bio-based polyurethane polymer electrolyte has been prepared from palm kernel oil and castor oil.[16-18]Bio-based polymer electrolytes were obtained higher ionic conductivity which has $1.53 \times 10^{-5}$ S/cm [16] for CMC based polymer and $1.3 \times 10^{-2}$ S/cm with chitosan polymer[17].

Jatropha oil is a non-edible oil which contains 78.9% unsaturated fatty acids consisting mainly of oleic acid and linoleic acid. This high degree of fatty acid makes it possible to undergo chemical modification to produce other polymers with specific properties. The unsaturated fatty acid can be functionalized to form epoxide, hydroxyl group or others. Jatropha oil has similar properties as that of palm oil and has the capacity to grow in marginal and common lands. The present research on jatropha oil is more focusing on biodiesel and medicinal purposes [18,19]. Nevertheless, jatropha oil can be a promising raw material to prepare polyols for the production of polyurethane. In this research, bio-based polyurethane acrylate was synthesized from jatropha oil-based polyol reacted with toluene 2,4-diisocyanate (TDI) and 2-hydroxyethylmethyl acrylate (HEMA). Solid polymer electrolyte was prepared by solution casting and cured with UV irradiation. The effect of different lithium salt concentration on the electrochemical properties, ionic conductivity, dielectric behaviour and thermal properties of the biopolymer electrolyte was investigated.

## 2. Experimental section

### 2.1. Materials

Jatropha seed oil was purchased from Biofuel Bionas, Malaysia. N, N-dimethylformamide (DMF) (99.5%) was obtained from R&M Chemicals, UK and tolylene-2,4-diisocyanate (TDI) (80%) was from ACROS Organics, USA. 2-hydroxyethyl methacrylate (HEMA) (97%) 1,6-hexaediol diacrylate (HDDA), lithium perchlorate ($LiClO_4$) and 2-hydroxy-2-

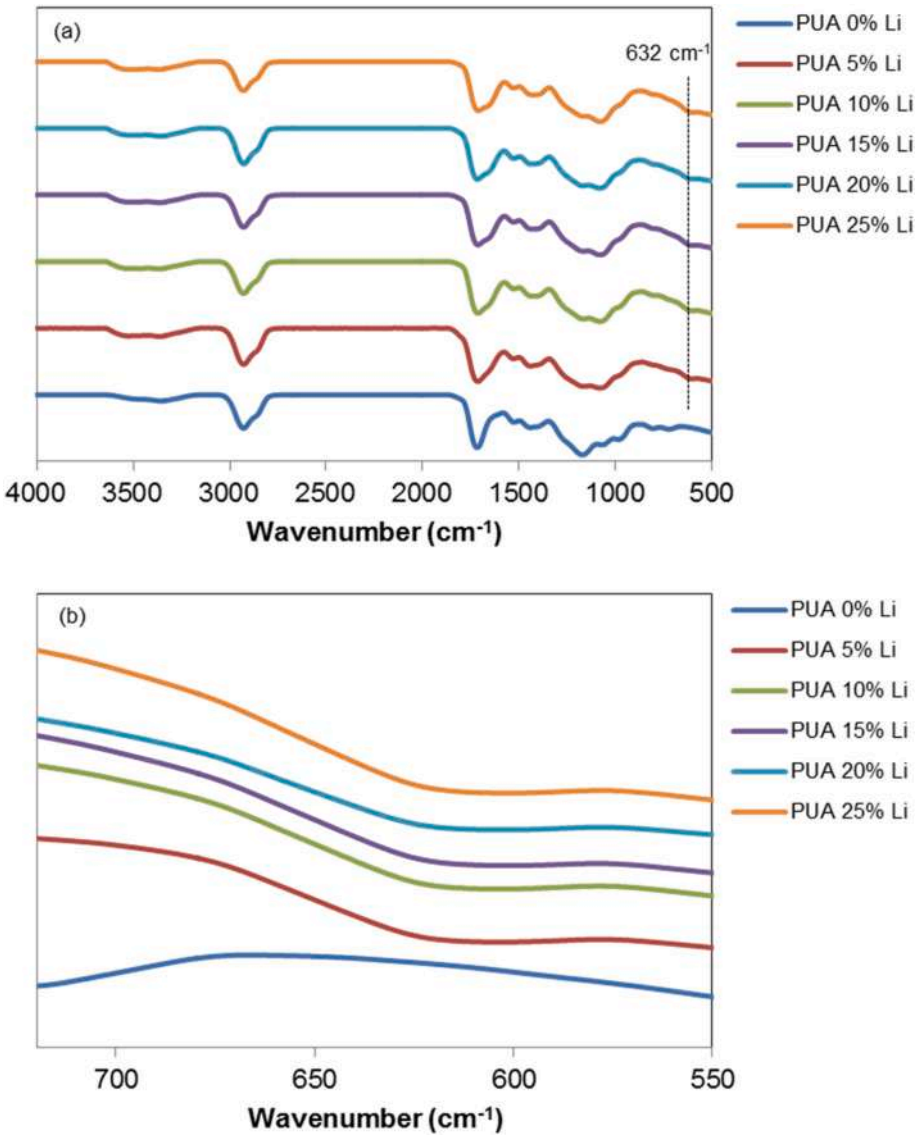


**Fig. 2.** FITR spectra of PUA electrolyte at various $LiClO_4$ content (0–25 wt.%) in the range of (a) 4000-500 $cm^{-1}$ and (b) 720-550 $cm^{-1}$.

methylpropiopropanone (Darocure) were purchased from Sigma-Aldrich, Germany. All chemicals were used as received.

### 2.2. Preparation of PUA oligomer

Polyol from jatropha seed oil (20 g) and DMF were added into a four necked bottom flask, stirred and refluxed under nitrogen atmosphere and heated to 60 °C. TDI was added drop wise into the mixture and stirred for 2 h. Then, the reaction was cooled down to 40 °C. HEMA was added drop wise into the reaction mixture over an hour and continuously stirred for another 2 h at 60 °C. TDI and HEMA were added with a ratio of 1:1:1 (polyol:TDI:HEMA). From time to time, DMF was added to the reaction mixture as diluent to control the viscosity of the reactant. Upon completion, a yellowish liquid product (PUA) was obtained. Fig. 1 schematically presents the preparation reaction of the PUA.

### 2.3. Preparation of PUA film electrolyte

PUA electrolytes were prepared by UV curing method. PUA, HDDA (monomer) and Darocure (photoinitiator) were mixed and stirred for 3 h in a close vial. Pure PUA without the addition of salt was used as the controlled parameter. For the PUA electrolyte, a calculated amount of lithium salt, in the range of 5–25 wt. % was used. Upon mixing, the lithium salt was dissolved in acetone. In another vial, PUA, HDDA and Darocure were mixed and stirred for 12 h. Then, these two solutions were mixed for another 12 h to obtain a homogenous solution. The electrolyte solution was casted on a Teflon mould and subjected to UV irradiation for 50 s. The fabricated SPE were stored in a desiccator.

### 2.4. Characterization

The FT-IR analysis was performed by Perkin Elmer Spectrophotometer model 1650. The electrolyte was analysed in the range of 4000 $cm^{-1}$ to 400 $cm^{-1}$, with a scanning resolution of 4 $cm^{-1}$. Thermal study was conducted by using TGA and DSC. TGA was performed with METTLER TA3000 from 50 °C to 700 °C at a heating rate of 10 °C/min under nitrogen atmosphere. Additionally, DSC analysis was conducted with METTLER TA300 under nitrogen atmosphere, from −50 to 150 °C (rate = 10 °C/min). The structure and crystallinity information of the polymer electrolyte was studied using XRD (D-5000 Siemen; 2θ: 5–35°; scan rate = 0.04° $s^{-1}$). The surface morphology of the sample was observed by SEM JEOL JSM-7600F. The sample was fractured in liquid nitrogen and sputtered with gold prior analysis at ambient temperature. Meanwhile, the ionic conductivity measurement was carried out by using EIS

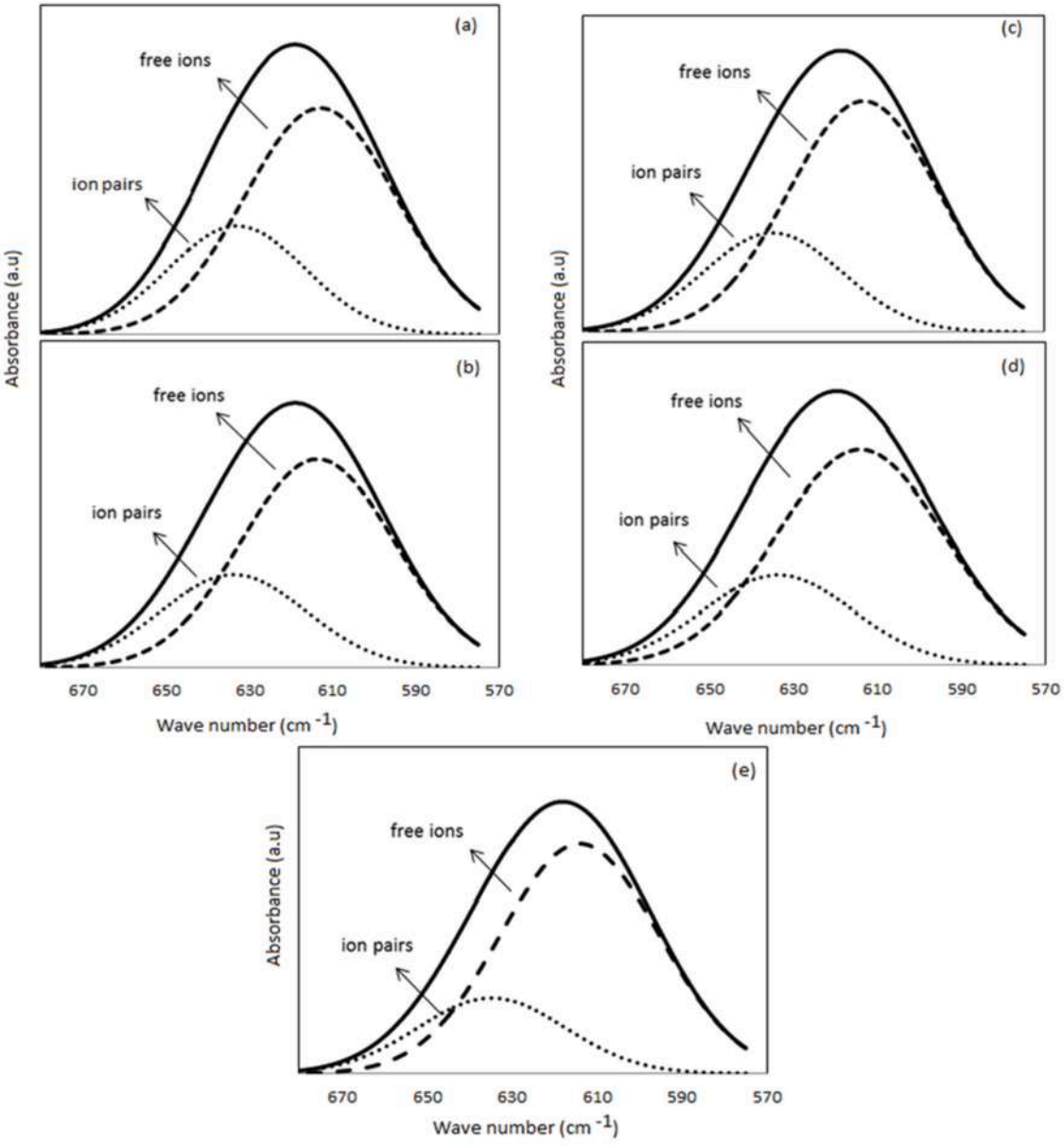


**Fig. 3.** FTIR deconvolution of peak between 680 and 570 $cm^{-1}$ of (a) 5, (b) 10, (c) 15, (d) 20, and (e) 25 wt.% of $LiClO_4$ in PUA solid polymer electrolytes.

HIOKI with an applied frequency from 50 Hz to 1 MHz at 100 mV amplitude at room temperature. Sample with 16 mm diameter disc-shaped was sandwiched between two stainless steel electrodes. The ionic conductivity at room temperature and at elevated temperature was obtained by calculating the bulk resistance from the impedance based on the following equation:

$$\sigma = \frac{l}{A \times R_b} \tag{1}$$

where $l$ represents the thickness of sample (cm), $A$ is the contact surface area ($cm^2$) and is the bulk resistance. From the impedance analysis, the number density (n), mobility (μ) and diffusion coefficient (D) of charge carriers can be calculated with the given the expression:

$$n = \left(\frac{m_{LiClO4}}{M_w} \times N_A\right) \frac{1}{V_T} \times \%f_{ion} \times 2 \tag{2}$$

$$\mu = \frac{\sigma}{ne} \tag{3}$$

$$D = \frac{\mu K_b T}{e} \tag{4}$$

where $m_{LiClO4}$ is the mass of $LiClO_4$, $M_w$ is the molecular weight, $N_A$ is Avogadro number, $V_T$ is the total volume, $e$ is the electron charge, $k_b$ is Boltzmann constant and $T$ is the temperature in kelvin. For the dielectric studies, the dielectric constant ($\varepsilon_r$), dielectric loss ($\varepsilon_i$), real electrical modulus ($M_r$), imaginary electrical modulus ($M_i$) and tan σ can be calculated by the following equations:

$$\varepsilon_r = \frac{Z_i}{\omega C_o \left(Z_r^2 + z_i^2\right)} \tag{5}$$

$$\varepsilon_i = \frac{Z_r}{\omega C_o \left(Z_r^2 + z_i^2\right)} \tag{6}$$

$$M_r = \frac{\varepsilon_r}{\left(\varepsilon_r^2 + \varepsilon_i^2\right)} \tag{7}$$

**Table 1**
Area percentage of free ions and ion pairs for PUA/$LiClO_4$ concentration in electrolyte system.

| Composition | Percentage area (%) | | Wave number ($cm^{-1}$) | |
|---|---|---|---|---|
| | Free ion | Ion pairs | Peak 1 | Peak 2 |
| PUA-5 wt.% Li | 66.90 | 33.10 | 613.36 | 632.91 |
| PUA-10 wt.% Li | 67.84 | 32.16 | 613.89 | 633.75 |
| PUA-15 wt.% Li | 69.28 | 30.72 | 613.89 | 634.70 |
| PUA-20 wt.% Li | 69.53 | 30.47 | 614.22 | 633.54 |
| PUA-25 wt.% Li | 74.56 | 25.44 | 614.41 | 634.70 |

$$M_i = \frac{\varepsilon_i}{(\varepsilon_r^2 + \varepsilon_i^2)} \tag{8}$$

$$\tan\delta = \frac{Z_r}{Z_i} \tag{9}$$

where $C_o = \varepsilon_o A/t$, $\varepsilon_o$ is the permittivity of free space and $\omega = 2\pi f$.

A linear sweep voltammetry (LSV) analysis was performed on the SS/SPE/Li electrodes (scan rate = 10mVs$^{-1}$; range = 0–7 V; room temperature). The cell was assembled in a glovebox with less than 0.1 ppm $H_2O$ and $O_2$. Princeton VersaSTAT-4 potentiostat and the polymer electrolytes were used for transference number measurement and which polarized under a fixed direct current (DC) voltage of 0.1 V. The value of $t_{ion}$ was calculated from the current versus time plot by using Wagner's polarization technique,

$$t_{ion} = 1 - \frac{I_{SS}}{I_o} \tag{10}$$

where $I_{SS}$ is the steady state current and $I_o$ is the initial current.

## 3. Results and discussion

### 3.1. Fourier transforms infrared

The FTIR spectra of PUA with different concentration of lithium perchlorate salts are presented in Fig. 2. The PUA polymer electrolytes displayed the characteristic stretching frequency of free and hydrogen bonded –NH (3800-3100 $cm^{-1}$), C═O (1750-1710 $cm^{-1}$), amine functional groups (C–N and N–H) (1550-1500 $cm^{-1}$) and C–O–C (1300-1000 $cm^{-1}$) [20]. Both the oxygen and nitrogen atoms interact with the lithium salt in the polymer electrolyte [21]. The absorption peak of free and H-bonded of –NH stretching of PUA have shifted and increase upon the introduction of lithium salt due to the interaction of $Li^+$ ions with the –NH groups.

The C═O signal of PUA without $Li^+$ gave an intense, strong and sharp peak at 1719-1712 $cm^{-1}$. The subsequent addition of shifted peak which wave number from 5 to 7 $cm^{-1}$ at 25 wt.% of lithium. This observation suggests that an interaction between the carbonyl group and lithium salt has weaken the C═O bond [22]. The peak between 1072 and 1173 $cm^{-1}$ was assigned for C–O–C stretching band for acrylate group. The urethane groups experienced only a marginal shift to a lower frequency. When salt was added, H bonded C–O–C groups became free due to an interaction of $Li^+$ ions with the ether oxygen and its ability to form H-bonds. The interaction of PUA solid polymer and $LiClO_4$ salt was also evident as a result of the formation of spectroscopically free $ClO_4^-$ recorded at 632 $cm^{-1}$ [23,24]. FTIR results prove that the introduction of Li salt into PUA results in a variety of interaction that can cause a change in the microstructure of the polymer.

FTIR deconvolution was used to study the interaction between PUA solid polymer and $LiClO_4$ salt [25, 26]. The area percentage of free ions and ion pairs can be calculated from the following formulae:

$$f_{ions}(\%) = \frac{A_f}{A_f + A_p} \times 100\% \tag{11}$$

$$P_{ions}(\%) = \frac{A_p}{A_f + A_p} \times 100\% \tag{12}$$

where $f_{ions}$ and $p_{ions}$ are free ions and ion pairs, respectively; while, $A_f$ and $A_P$ are the area of free ions and ion pairs, respectively. According to the previous report [27], the recorded peaks at 600 $cm^{-1}$ and 650 $cm^{-1}$ were assigned to the free ions and ion pairs of $ClO_4^-$, respectively. The spectra measured from 680 $cm^{-1}$ to 570 $cm^{-1}$ were fitted by using non-linear least squares and the results were shown in Fig. 3. Herein, the peaks at 613 and 614 $cm^{-1}$ are assigned to the free ions, while the ion pairs of $ClO_4^-$ were found at 633 and 634 $cm^{-1}$. The peak deconvolution

**Table 2**
Thermal analysis of the PUA electrolytes at different percentages of $LiClO_4$.

| Composition | $T_{d1}$ (°C) | $T_{d2}$ (°C) | Residue (%) |
|---|---|---|---|
| PUA-0 wt.% Li | 254 | 416 | 0.0 |
| PUA-5 wt.% Li | 285 | 404 | 0.0 |
| PUA-10 wt.% Li | 312 | 428 | 12.1 |
| PUA-15 wt.% Li | 319 | 428 | 18.5 |
| PUA-20 wt.% Li | 296 | 462 | 16.6 |
| PUA-25 wt.% Li | 305 | 448 | 17.3 |

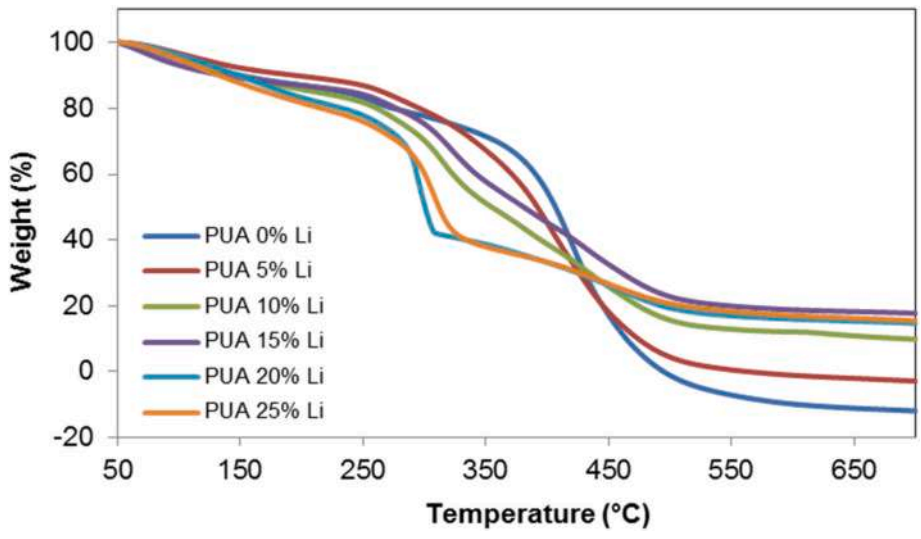


**Fig. 4.** TGA thermograms of PUA electrolyte with varied $LiClO_4$ composition.

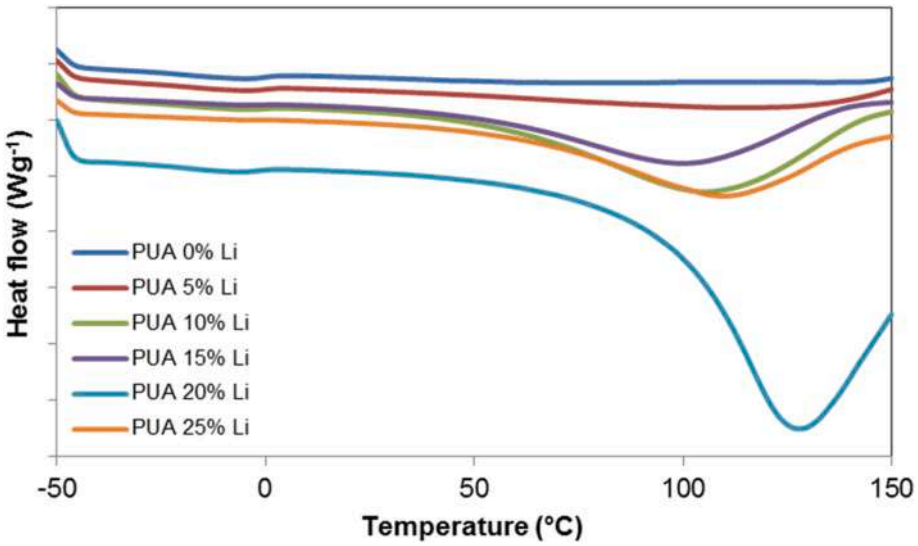


**Fig. 5.** DSC curves of the PUA-$LiClO_4$ electrolytes.

**Table 3**
$T_g$ and $T_m$ of the PUA-$LiClO_4$ electrolytes.

| Composition | $T_g$ (°C) | $T_m$ (°C) |
|---|---|---|
| PUA-0 wt.% Li | −18.1 | - |
| PUA-5 wt.% Li | −15.7 | 115.2 |
| PUA-10 wt.% Li | −15.8 | 105.0 |
| PUA-15 wt.% Li | −15.7 | 99.6 |
| PUA-20 wt.% Li | −20.4 | 125.3 |
| PUA-25 wt.% Li | −15.1 | 108.9 |

and percentage of free ions and ion pairs can be calculated by equation (11) and equation (12) and the area percentage was summarized in Table 1. Based on the tabulated results, the area percentage of free ions increased with the percentage increment of $LiClO_4$ salt doped into PUA. The ion dissociation of PUA (5% $LiClO_4$) was 66.90% up to a maximum of 74.56% for PUA (25% $LiClO_4$). This suggests that addition of $LiClO_4$ salt has resulted in the favourable formation of free ions and increased the charge carries that would enhance ionic conductivity [25]. However, the area percentage of ion pairs depicted a decreasing trend from 33.10% (5% $LiClO_4$) to 25.44% (25% $LiClO_4$). The increasing amount of $LiClO_4$ salt added unto PUA solid polymer electrolyte resulted in a higher degree of free ion mobility with the accompanying tendency for negative charge generation. Therefore, the dissociation of ion will decrease as the formation of ion pairs decreases.

### 3.2. *Thermogravimetric analysis*

The TGA thermograms of pure PUA and PUA with different percentages of $LiClO_4$ salt are shown in Fig. 4. The weight loss of 5–15 wt.% at below 100 °C is due to the loss of water and solvent present in the polymer electrolyte. The weight loss due to water increased as the percentage of hygroscopic Li salt increased. The thermal decomposition stage ($T_d$) of pure PUA and PUA with $LiClO_4$ was observed at temperature region of 250–350 °C and 350–500 °C for first decomposition stage ($T_{d1}$) and second decomposition stage ($T_{d2}$), respectively (Table 2). $T_{d1}$ of PUA was ascribed to the degradation of urethane linkage while the degradation of polyether contributed to $T_{d2}$ [22]. The addition of lithium to polymer electrolyte contributes to the early decomposition

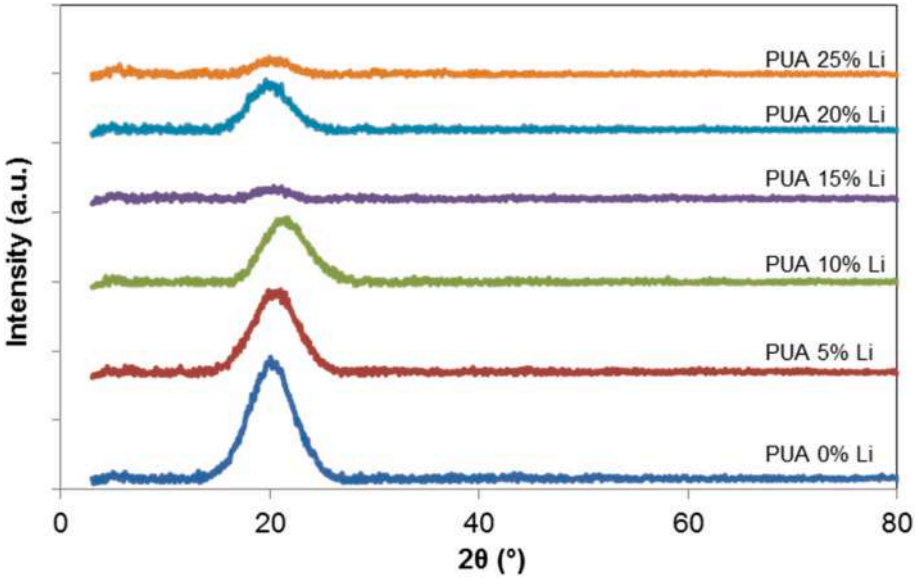


**Fig. 6.** XRD patterns of PUA-$LiClO_4$ electrolytes at different salt concentrations.

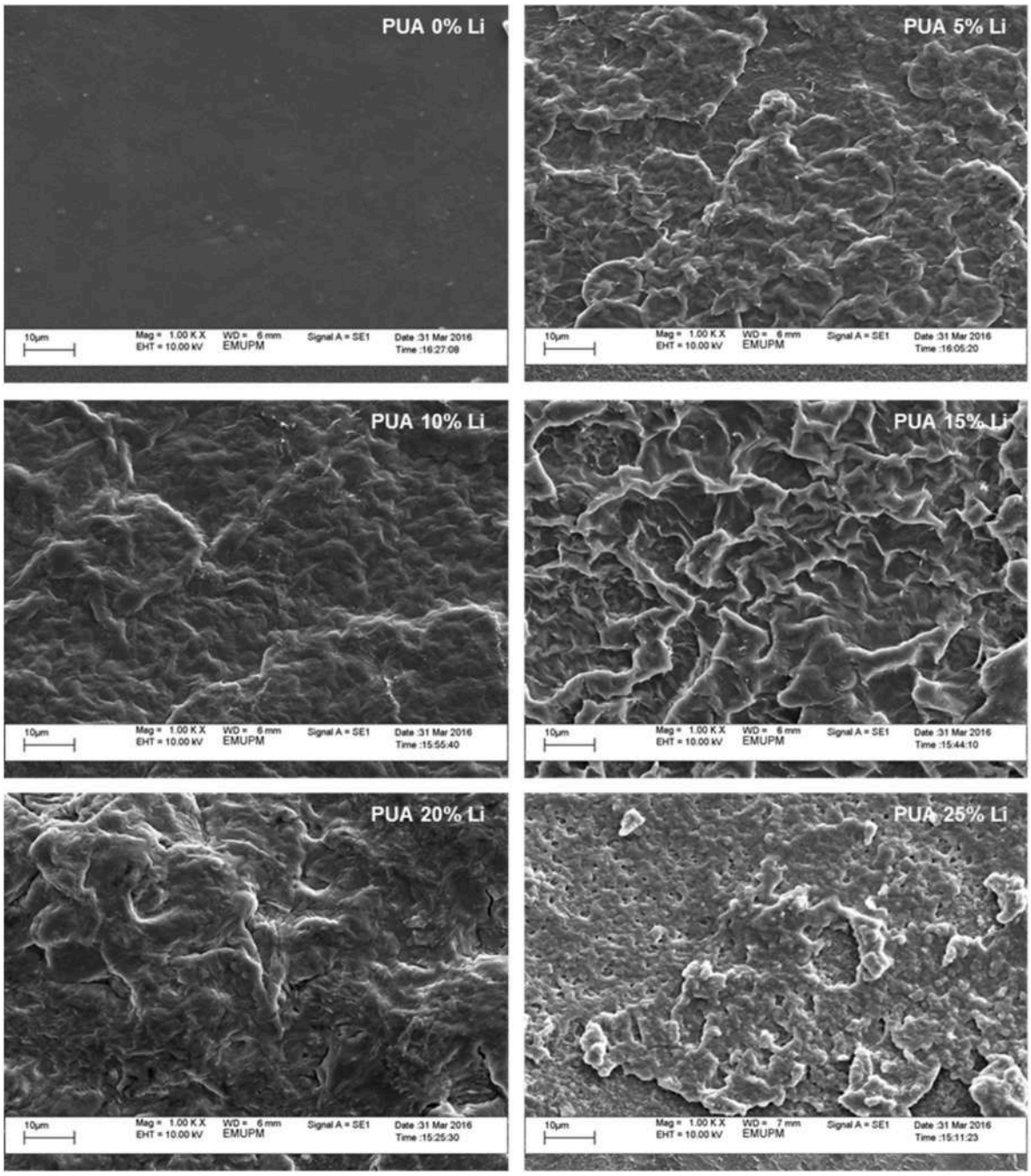


**Fig. 7.** Morphology of the PUA electrolytes at different $LiClO_4$ salt concentrations.

than pure PUA. The interaction of $Li^+$ ions with the oxygen atoms of polymer electrolyte weaken the C═O bond. Besides, the introduction of lithium salt into PUA has decreased the percentage loss of mass upon heating. Lithium salt may promote early decomposition. As the amount of lithium increases, the percentage loss of mass in the polymer is lowered. Moreover, the decomposition of urethane linkage at lower temperature corroborates the weakening of C═O bond and decreases the electron density due to interaction of $Li^+$ with the oxygen atoms [26]. The increase in lithium salt concentration has affected the thermal stability of the polymer electrolyte attributed to the reduction of crosslink density of the polymer. It is observed that the PUA is degraded completely while the polymer electrolyte was left about 12–19 wt. %. The systematic addition of salt dopant (5–25 wt. %) has also escalated the polymer electrolyte residue seen beyond 600 °C.

### 3.3. Differential scanning calorimetry

The undoped PUA sample exhibited recorded a glass transition temperature at −18.1 °C which corresponded to the one reported by previous study [28]. Each sample of the polymer electrolyte showed one $T_g$ and one endothermic melting peak, $T_m$ except for PUA (0% $LiClO_4$). The crystalline peak of the exothermic of PUA was not observed by the DSC analysis. The $T_g$ of the polymer electrolytes are higher than the undoped PUA except for the PUA with 20 wt. % of Li salt (Fig. 5 and Table 3). The $T_g$ of the polymer mainly depends on intermolecular interaction and chain flexibility. The lower values of $T_g$ with the addition of 20 wt. % salt was attributed to the plasticizing effect of the Li salt in the polymer matrix. The introduction of $Li^+$ ions elevated the segmental motion hence lowered the $T_g$ of polymer electrolyte [29,30]. The introduction of $LiClO_4$ has caused the effective packing of polymer

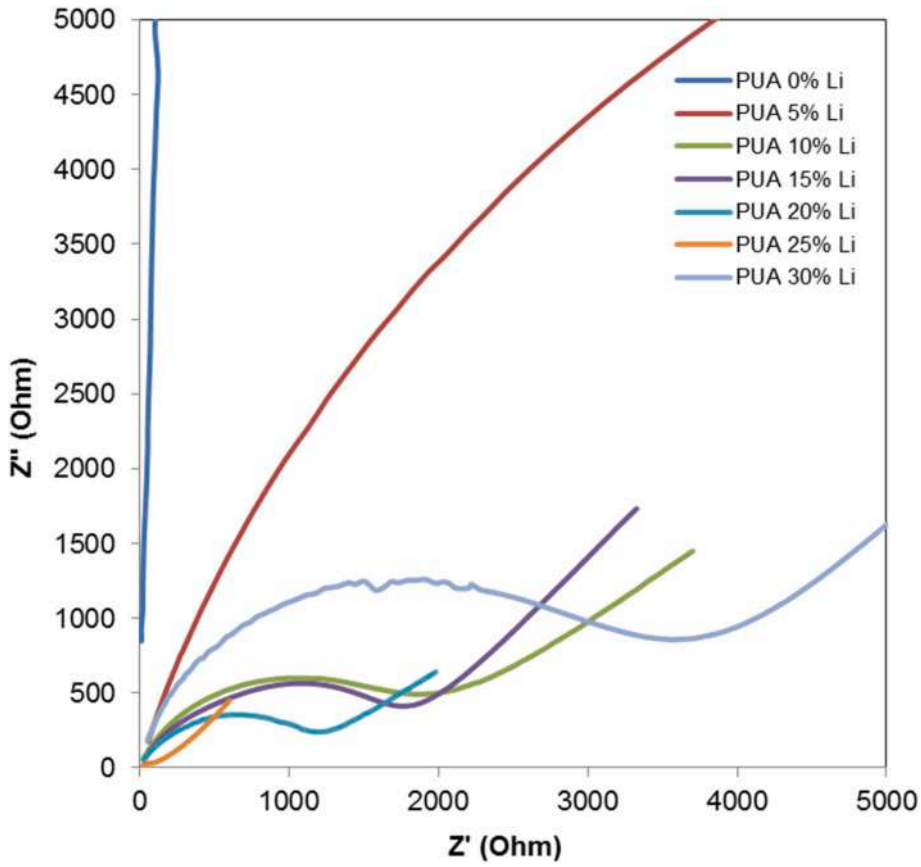


**Fig. 8.** Impedance plots of PUA electrolyte.

**Table 4**
Ionic conductivity of the PUA-$LiClO_4$ electrolytes.

| Composition | Conductivity (S $cm^{-1}$) |
|---|---|
| PUA-0 wt.% Li | $2.61 \times 10^{-11}$ |
| PUA-5 wt.% Li | $3.66 \times 10^{-7}$ |
| PUA-10 wt.% Li | $5.57 \times 10^{-6}$ |
| PUA-15 wt.% Li | $3.95 \times 10^{-6}$ |
| PUA-20 wt.% Li | $9.36 \times 10^{-6}$ |
| PUA-25 wt.% Li | $6.40 \times 10^{-5}$ |
| PUA-30 wt.% Li | $3.25 \times 10^{-6}$ |

chains into the solid-state crystals and produced a semi-crystalline material [31]. A single glass transition was observed since the incorporation of polyol in the PUA is presumably small. Hence, the separation of the soft-hard segment phases is limited [32]. Likewise, the melting temperature of polymer electrolyte displayed similar trend.

Based on Table 3, the $T_m$ values decreased accordingly with the increasing amount of $LiClO_4$ 5–15 wt%. The lower $T_m$ temperature upon the addition of $LiClO_4$ salt suggests that the polymer salts segment became less rigid in the amorphous phase which is supported by the XRD analysis which will be discussed in the following section. The decreasing $T_g$ and $T_m$ of the polymer host was also related to the increase in the ionic conductivity of the polymer electrolyte. The incorporation of the salt into PUA caused the weakening of the dipole-dipole interaction between the PUA chains and hence, promotes ions mobility through the polymeric chain network when an electric field [20]. Nevertheless, the addition of salt at 20 wt. % has higher $T_m$ and lower $T_g$ attributed to a stronger Li-polymer matrix interaction. However, it was found that the subsequent increase of 25 wt. % salt give rise to a decreased $T_m$ which suggests that the addition of salt weakened the dipole-dipole interactions. The further addition of Li salt restricted the PUA chains and reduces the bonding interactions between network chains.

Typically, there are three major types of interaction involving the polymer electrolyte. Firstly, the interaction of the ether oxygen with the $Li^+$ ions, leads to the formation of transient crosslinks between the polyether chains via the $Li^+$ ions, as a result restricts the segmental motion. The second type of interaction involves the –NH (urethane), carbonyl groups and the $Li^+$ ions conforming to an inter or intra molecular crosslink. The third type of interlinkage includes the ether-urethane interaction with the $Li^+$ ions which leads to the mixing of phases involving the hard and soft segments. Besides, the oxygen atoms present in the acrylate groups may also coordinate with $Li^+$ ions. The interaction of $Li^+$ happens within the ether oxygen and possibility through the oxygen of acrylate group that would likely increase the $T_g$ of the hard segment. This information suggests that the addition of salt promotes the amorphous characteristics of PUA.

### 3.4. X-ray diffraction

The XRD analysis was carried out to study the crystallinity behavior of the polymer materials. Fig. 6 shows the XRD pattern of PUA and PUA electrolyte. The XRD pattern of PUA and PUA electrolyte shows a broad hump within 15°–25°. There was no crystalline peak of Li referred to and reported by Ulaganathan et al. [33] and observed in XRD pattern which indicates that there is complete dissolution of Li salts in polymer matrices [34]. Besides, the existence of broad hump indicates that the PUA and PUA electrolyte are amorphous phase. The intensity of the peak decreases and the broadening area under the peak becomes smaller with the addition of Li salts. This implies that the amorphous nature of the film increases with the increase in the concentration of lithium. The crystallinity of polymer reduces whenever lithium salt was added known as favourable condition for conductivity enhancement [35]. The physical crosslinking contributed by Li salt stronger than the force attraction

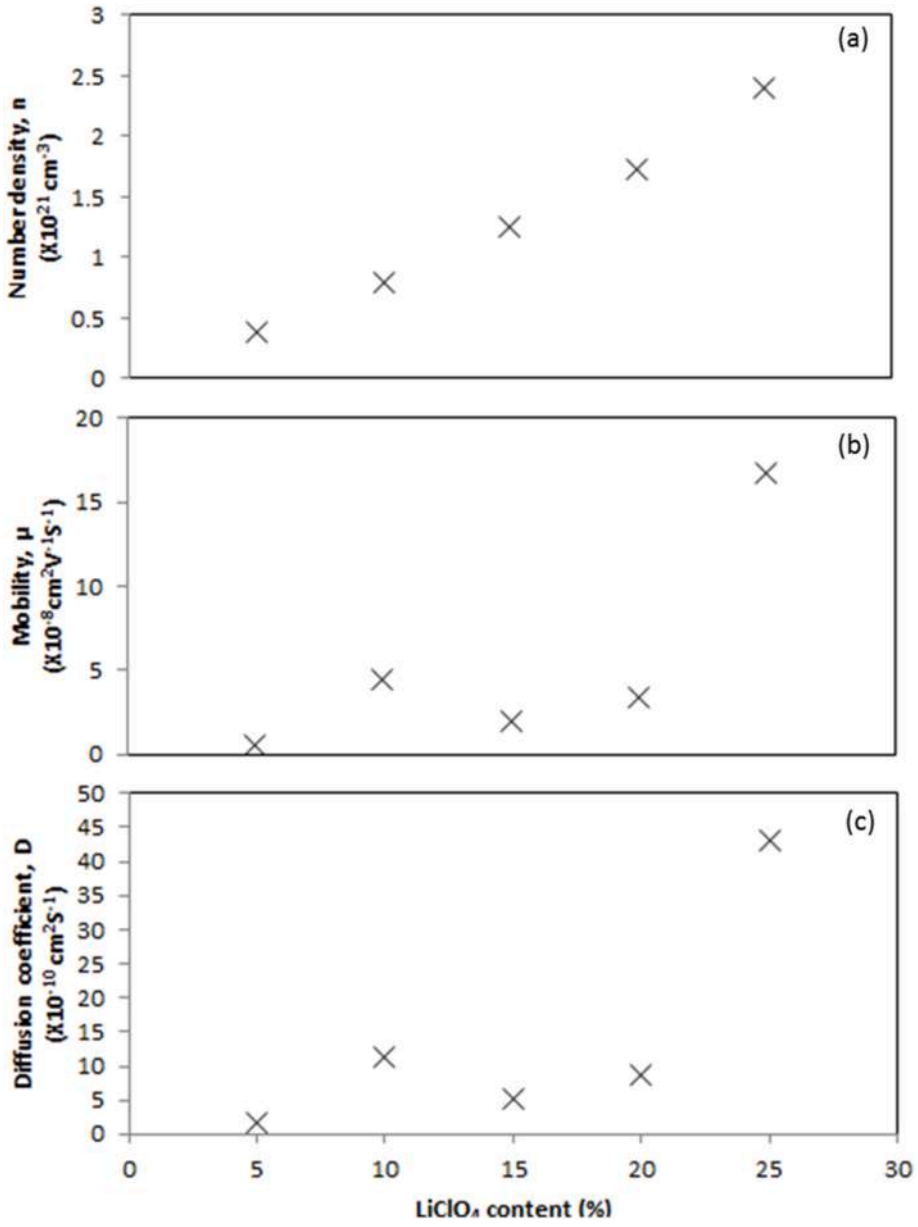


**Fig. 9.** (a) Number density, (b) mobility and (c) diffusion coefficient of charge carriers for PUA solid polymer electrolyte with different Li content.

between the polymer chains. The increase in the amorphous nature causes a reduction in the energy barrier to the segmental motion of the polymer electrolyte. Hence, improving ionic mobility and enhancing ionic conductivity of polymer electrolyte at room temperature [34].

The amorphous properties of polymer give a significant reason for the increment of ionic conductivity which might be due to the free volume created by the continuous segmental motion of polymer chain. This helps ion migration and facilitates the movement of ions [36]. The amorphous nature of polymer electrolyte was responsible for reducing $T_g$ value as discussed in DSC analysis. It was shown that the more amorphous polymer has a low $T_g$ which explained that the low $T_g$ in amorphous phase has caused the polymer chains to produce faster bond rotations and segmental motion, hence giving a better ionic mobility to the polymer electrolyte.

### 3.5. Morphology analysis

Morphology studies the fractured surface of the PUA added with Li salt shows in Fig. 7(a–f). The SEM micrograph Fig. 7(a) shows the homogenous surface of pure PUA as observed. For PUA with and without salt, there were no phase separations observed meaning there are intermolecular interaction between oxygen atom and host polymer [37]. Topological texture of PUA changed from smooth to rough and brighter surface with addition of lithium salt. Fig. 7(f) has micro size pores affecting the transporting properties of $Li^+$ ions by increasing the surface area. Hence, 25 wt. % of lithium salt has higher conductivity and the blacker region in the SEM micrograph exhibited an amorphous phase while crystalline phase is contributed by the lighter region in the polymer electrolyte system [16]. Amorphous region helps migration of ions in the polymer, hence increasing the conductivity.

### 3.6. Ionic conductivity, ion transport properties and dielectric study

The impedance spectroscopy study was conducted to study the ionic conductivity of PUA polymer electrolyte. Fig. 8 shows the impedance plots of the PUA electrolytes and the ionic conductivity value is displayed in Table 4. Based on Fig. 8, the curve of all PUA electrolytes with the salt are in similar shape with the arc (high frequency) and straight

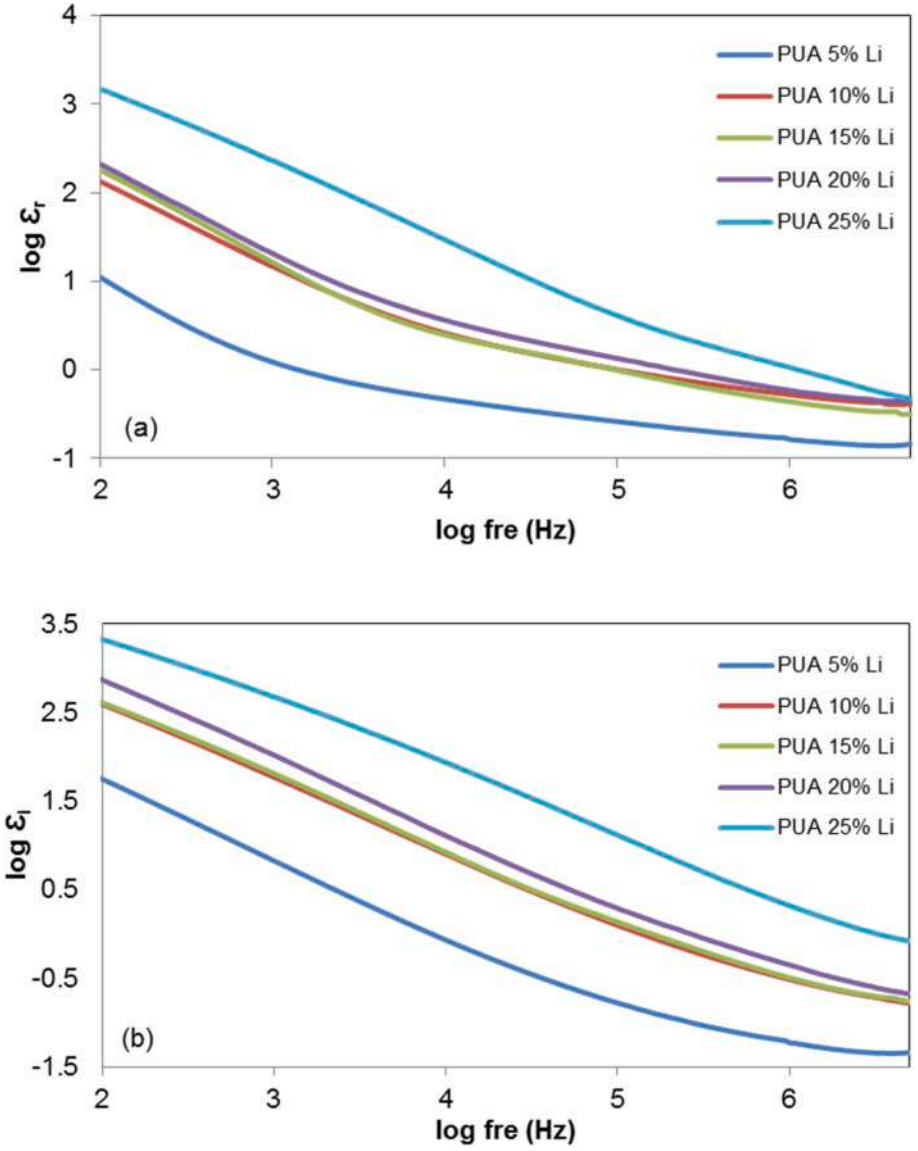


**Fig. 10.** Plots of (a) log dielectric constant and (b) log dielectric loss against log frequency of PUA-$LiClO_4$ at different salt concentrations.

line (low frequency) regions. It is established that the resistance of a cell system is composed of the bulk resistance, $R_b$ and interfacial resistance, $R_i$. The increase of lithium salt has resulted in a smaller bulk resistance [22]. In the relatively low frequency region, the diffusion of active species determines the impedance response. As the frequency increases, the charge transfer reaction during potential oscillation decreases so that the influence of the diffusion of active species on the impedance response decreases [26]. From Table 4, the ionic conductivity increased as $LiClO_4$ added increased from 5 wt. % up to 25 wt. %. The PUA electrolyte with 25 wt. % of lithium salt showed the highest conductivity of $6.4 \times 10^{-5}$ S $cm^{-1}$ at r.t. which has increased by six orders compared to the pure PUA. As the percentage of salt increases, the ionic conductivity is increased until it peaked at an optimum value, $6.4 \times 10^{-5}$ S $cm^{-1}$. However, the conductivity decreased with the addition of Li salt beyond the optimum point. This observation is related to the ion pair formation that lowers the concentration of free ions in the solutions. Thereafter, the PUA (25 wt. % of $LiClO_4$) was subsequently used for further analyses.

It was found that the augmentation of ionic conductivity will also increase the number density, mobility and diffusion coefficient of charge carriers as shown in Fig. 9. The number density of charge carriers increased linearly with the content of $LiClO_4$ content from $0.376 \times 10^{21}$ to $2.390 \times 10^{21}$ $cm^{-3}$ [38,39]. The ionic conductivity was dominated by the increase of number density of charge carriers with 74.56% free ions. Furthermore, the mobility of charge carriers improved gradually up to $16.7 \times 10^{-8}$ $cm^2V^{-1}s^{-1}$ (PUA 25% Li). Both, the mobility and diffusion coefficient of charge carriers were enhanced as the flexibility of PUA SPE increased [38].

Accordingly, we have compared the variation of log dielectric constant (log $\varepsilon_r$) and log dielectric loss (log $\varepsilon_i$) against log frequency for the doped-PUA (5–25% Li) at 26 °C (Fig. 10). Higher values of log $\varepsilon_r$ and log $\varepsilon_i$ were present at lower frequency ca. 2 Hz as result of ion polarization [40]; while, at higher frequencies, the log $\varepsilon_r$ and log $\varepsilon_i$ decreased as there was no excess of ion diffusion in the field direction and engender the rapid periodic reversal of electric field [41]. When more $LiClO_4$ salt was added into PUA solid polymer electrolyte, consequently, the log dielectric constant and log dielectric loss were likewise increased from PUA 5% Li to 25% Li. The increasing value of log $\varepsilon_r$ and log $\varepsilon_i$ were dominated by the charge carrier density, $n$ [42]. As the values of $n$ increased, the number of free ions increased too and facilitated the elevation of ionic conductivity.

The real ($M_r$) and imaginary ($M_i$) parts of the electric modulus versus log frequency for different concentration $LiClO_4$ was shown at Fig. 11. From Fig. 11, it was observed that values for $M_r$ and $M_i$ were increased at higher frequency about 6.5 Hz and 5.0 Hz respectively. Based on that,

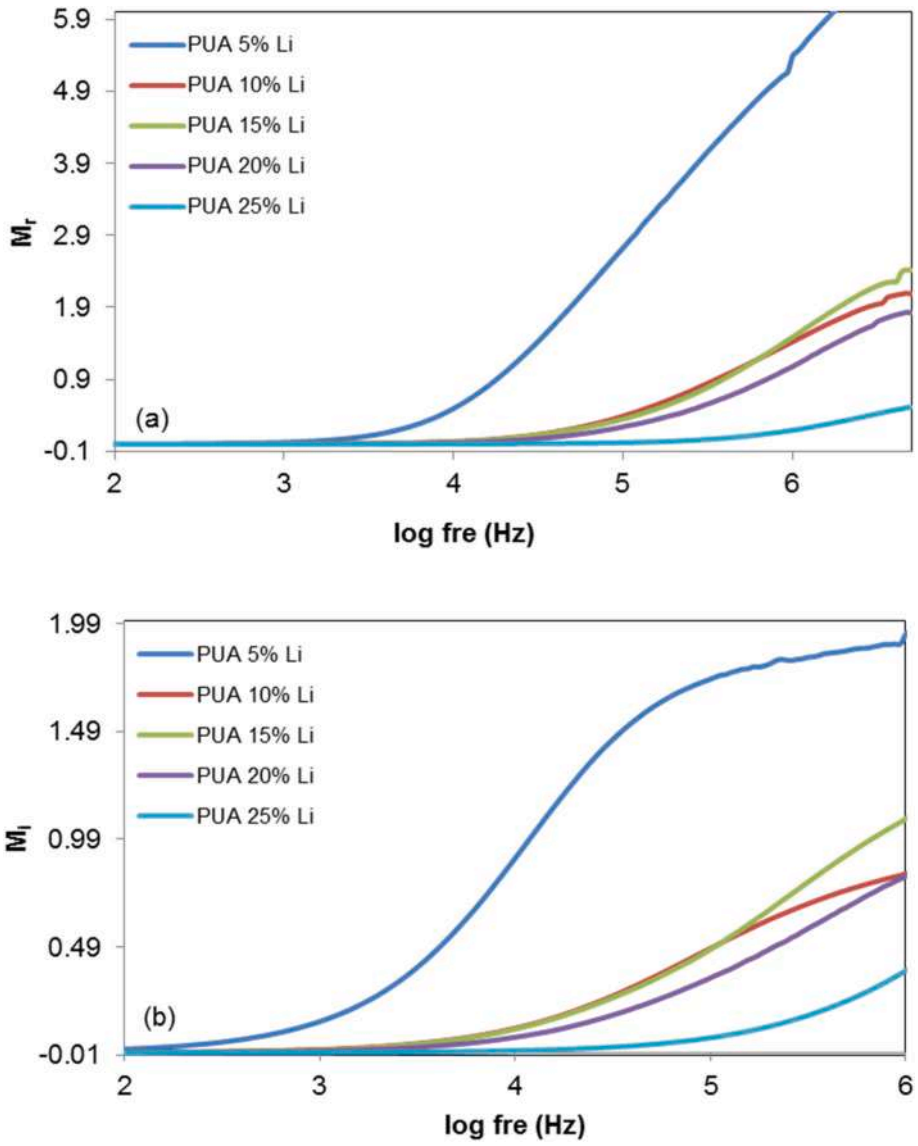


**Fig. 11.** Plots of (a) real part ($M_r$) and (b) imaginary part ($M_i$) electrical modulus against log frequency for PUA 5%–25% Li.

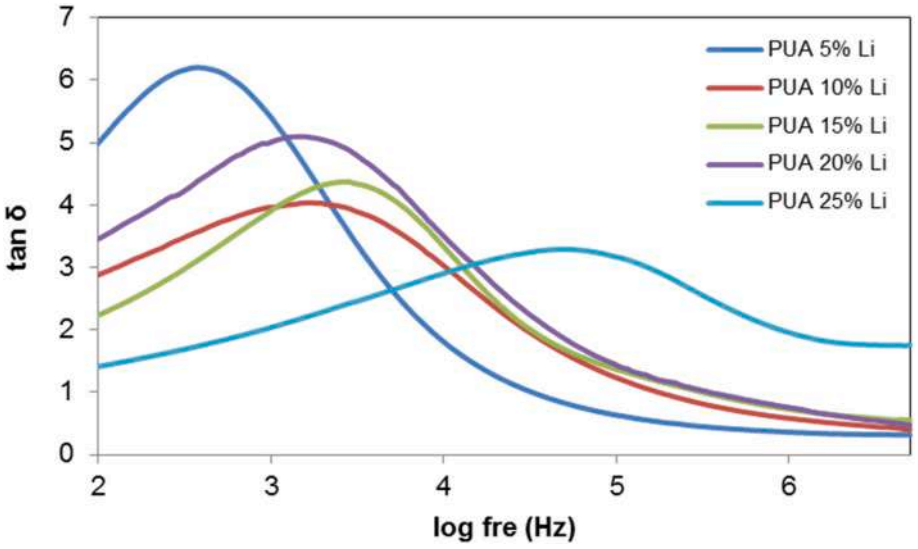


**Fig. 12.** Tan δ versus log frequency for PUA 5%–25% Li.

**Table 5**
Relaxation parameter for different percentage of Li doped into PUA SPE.

| Composition | Maximum peak (Hz) | $\tau$ ( $\times 10^{-4}$ s) |
|---|---|---|
| PUA-5 wt.% Li | 2.59 | 25.70 |
| PUA-10 wt.% Li | 3.29 | 5.13 |
| PUA-15 wt.% Li | 3.43 | 3.72 |
| PUA-20 wt.% Li | 3.21 | 6.17 |
| PUA-25 wt.% Li | 4.69 | 0.20 |

the PUA solid polymer electrolyte samples can be said that it was an ionic conductors [43]. This was because it consisted of charge carriers that can help to increase the ionic conductivity. The $M_r$ and $M_i$ indicated that both had zero values with a present of tail at lower frequency. The tail determined that there was capacitance associated with the electrodes [40,43]. This was due to the effect of polarization was very tiny [26] as there was capacitance associated with electrolyte.

A graph of tan θ against log frequency was plotted in Fig. 12. Based on Equation (9), the relaxation time (τ) can be calculated for different percentage of Li doped into PUA solid polymer electrolyte. In Fig. 12, the peaks were shifted toward the right (higher frequency) with increased the percentage of Li. As percentage of Li doped into PUA SPE increased, the number of free ions increase, and it will lead to increase of ionic conductivity. From Table 5, the relaxation time taken was decreased [41] as the peaks shifted toward right at higher frequency. PUA 25% Li seem to have the lowest value of τ of $0.204 \times 10^{-4}$ s that had the highest ionic conductivity which was $6.40 \times 10^{-5}$ S $cm^{-1}$.

### 3.7. Temperature dependence study

The 25 wt.% $LiClO_4$ PUA electrolyte that have maximum ionic conductivity at r.t. was studied for conductivity at ambient temperature up to 100 °C. The temperature dependence on ionic conductivity was studied to analyse the mechanism of ion transportation in polymer electrolytes. The log σ versus 1000/T grafted in Fig. 13 showed a linear plot well-fitted with Arrhenius theory as follows:

$$\sigma = A\, exp\left(\frac{-E_a}{kT}\right) \tag{13}$$

where A is a constant which is proportional to the amount of charge carriers, $E_a$ is activation energy, $k$ is Boltzmann constant and $T$ represents the absolute temperature in K. The graph showed that the ionic conductivity was increased as temperature increased. When the

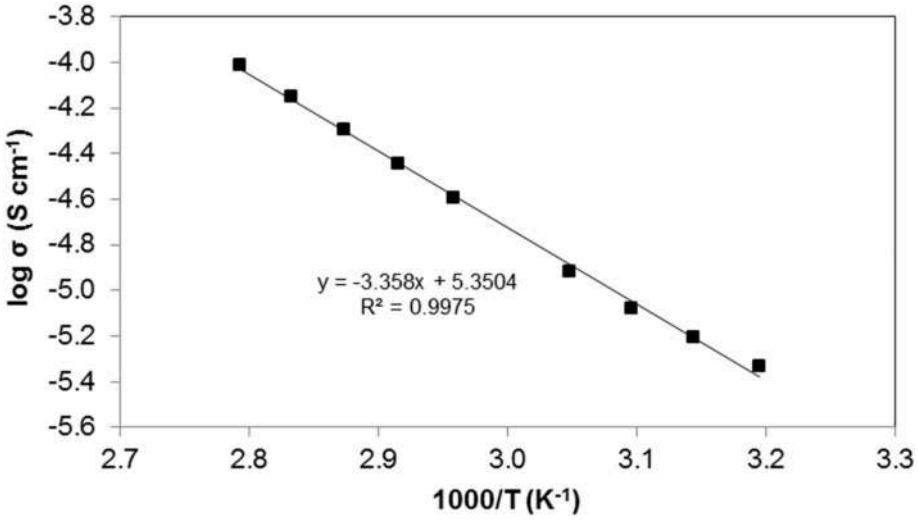


**Fig. 13.** Temperature dependence of ionic conductivity of PUA-$LiClO_4$ electrolytes.

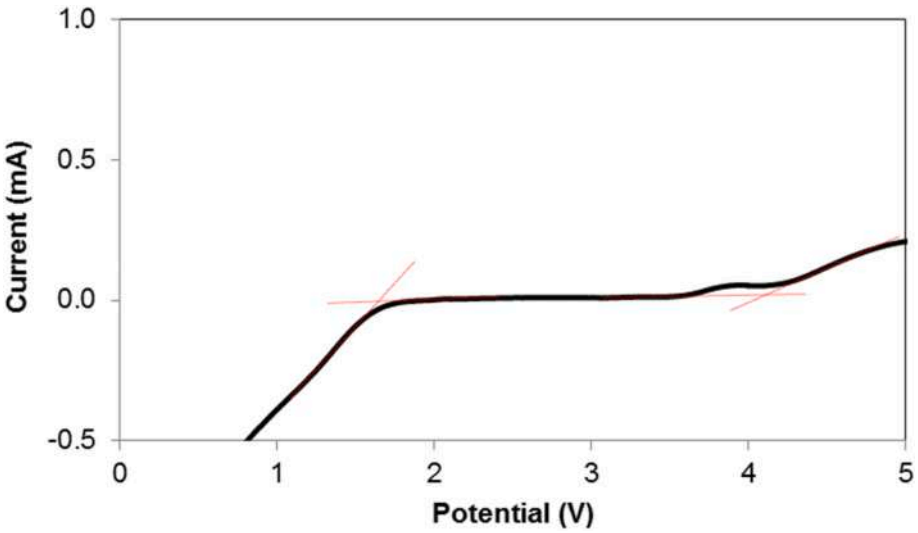


**Fig. 14.** Linear sweep voltammetry of PUA-25 wt.% $LiClO_4$.

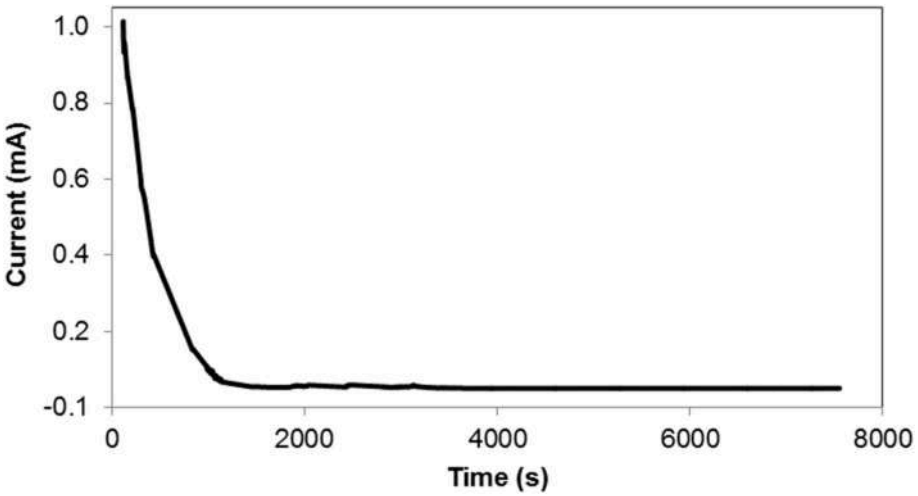


**Fig. 15.** Normalized current versus time of PUA-25 wt.% $LiClO_4$.

temperature increased, the free ions in polymer increased hence increased the ionic conductivity of PUA electrolyte. The pseudo-activation energy, $E_a$ of polymer electrolyte was determined from the Arrhenius graph. $-E_a/k$ denotes the graph slope and the activation energy is 0.29 eV. The value of activation energy is related to the ionic conductivity. The higher ionic conductivity has a lower activation energy and vice versa. This indicated that the higher conducting electrolyte requires only a smaller energy to start a migration process [20]. Based on a reported study, the lower $E_a$ provides a smaller band gap which allows the conducting ion to move more easily as a free ion-like state, hence increases ionic conductivity. Besides, lower $E_a$ is required for the migration of ions and higher in the conduction process of the sample. Since migration of ions is affected in electrolyte with a lower $E_a$ facilitates ionic movement, which then increases conductivity [44].

### 3.8. Linear sweep voltammetry analysis

The electrochemical stability window of polymer electrolyte was obtained by the linear sweep voltammetry technique. The sample was sandwiched between SS/SPE/Li metal electrode at ambient temperature. Fig. 14 shows LSV for 25 wt. % $LiClO_4$ PUA electrolyte as a function of voltage. The onset of current determines the electrolyte breakdown voltage. The maximum working voltage ($V_{max}$) of PUA with Li salt extends to about 4.0 V. The working potential range for practical lithium rechargeable batteries is generally between +1.8 and + 3.5 V vs. $Li/Li^+$ [45]. Based on the results, these PUA electrolytes have electrochemical stability window widen to 4.0 V which is similar with other study [46]. The good electrochemical stability of PUA electrolyte suggested that PUA electrolyte can be used as a candidate electrolyte material for energy storage devices such as for rechargeable lithium polymer batteries which have working voltage widen to 4.0 V.

### 3.9. Transference number

The mobility of ionic species is important parameter to be considered in designing polymer electrolyte. The ionic transference number for PUA electrolyte with 25 wt.% of $LiClO_4$ has been determined by the D.C. polarization method. The current was observed as a function of time on application of a D.C. potential across SS/SPE/SS cell. The normalized current versus time plots was shown in Fig. 15 for PUA-$LiClO_4$ polymer electrolyte. When D.C. potential was applied to across the test cell, the current decays immediately occur to lower steady state. This is obviously showed by gradients formed due to the non-unity transference number of lithium ions in polymer electrolytes. The initial total current was decreased with time due to depletion of ionic species in electrolyte. The cell was polarized and current flows when electron migrates across the electrolyte and interfaces in a steady state condition. If the electrolyte is primarily ionic, the ionic currents through an ion-blocking electrode fall rapidly with time [42]. The values of the cation transference number for PUA electrolyte is 0.99. In PUA electrolyte, cation can coordinate with oxygen and nitrogen in PUA and with oxygen in $ClO_4^-$.

## 4. Conclusion

PUA electrolyte films were prepared by varying lithium salt from 5 to 25 wt. % and the addition of 25 wt. % lithium salt exhibited the highest ionic conductivity of $6.4 \times 10^{-5}$ S $cm^{-1}$ at a room temperature six magnitude higher compare to the pure PUA. The increase in the ionic conductivity is due to an increase in charge carrier ions and amorphous phase of polymer electrolyte film which is confirmed by XRD, SEM analysis and DSC analysis. Besides, the interaction of lithium salt with polymer matrix was supported by FTIR. Deconvulation of the FTIR spectra shows that the ionic conductivity was dominated by the increase of number density of charge carriers with 74.56% free ions. The temperature dependence on polymer electrolyte followed Arrhenius theory. The cation transference number achieved was 0.99, whereas the electrochemical stability exhibited 4.0 V. Overall, the PUA-LiClO4 electrolytes shows favourable properties and has a potential to be applied in battery of electrochemical devices.

## Authors statement

Conceptualization, Min Min Aung.; methodology, Min Min Aung.; formal analysis, Tuan Syarifah Rossyidah Tuan Naiwi. Chai Kai Ling and Azizan Ahmad.; investigation, Min Min Aung and Marwah Rayung.; resources, Tuan Syarifah.; writing—original draft preparation, Tuan Syarifah and Min Min Aung.; writing—review and editing, Wun Fui Mark Lee, Emma Ziezie Mohd Tarmizi and Nor Azah Abdul Aziz.; supervision, M.M.A. and Azizan Ahmad funding acquisition, M.M.A. All authors have read and agreed to the published version of the manuscript.

## Declaration of competing interest

The authors declare the following financial interests/personal relationships which may be considered as potential competing interests: Min Min Aung reports was provided by Putra Malaysia University. Min Min Aung reports a relationship with Putra Malaysia University that includes: employment.

## Acknowledgement

The authors would like to acknowledge Universiti Putra Malaysia for a grant of financial support (GP-IPB/9532000).

## References

[1] L. Li, X. Yang, J. Li, Y. Xu, A novel and shortcut method to prepare ionic liquid gel polymer electrolyte membranes for lithium-ion battery, Ionics 24 (3) (2018) 735–741.
[2] H. Xu, F. Qiu, Y. Wang, W. Wu, D. Yang, Q. Guo, Progress in organic coatings UV-curable waterborne polyurethane-acrylate: preparation, characterization and properties, Prog. Org. Coating 73 (1) (2012) 47–53.
[3] E.J. Lee, H.H. Park, Y.H. Lee, K.G. Kim, Y.U. Jeong, S.Y. Kim, H.D. Kim, Poly (urethane acrylate)-based gel polymer films for mechanically stable, transparent, and highly conductive polymer electrolyte applications, J. Appl. Polym. Sci. 134 (2018) 26.
[4] S.A.M. Noor, A. Ahmad, I.A. Talib, M.Y.A. Rahman, Effect of ZnO nanoproperties filler concentration on the properties of PEO-ENR50-$LiCF_3SO_3$ solid polymeric electrolyte, Ionics 17 (5) (2011) 451–456.
[5] B.Y. Hicham, G.C. Oihane, L. Nerea, D. Shanmukaraj, A. Michel, Cross linked solid polymer electrolyte for all solid state rechargeable lithium batteries, Electrochim. Acta 220 (2016) 587–594.
[6] P. Simona, I. Smaranda, I. Gheorghe, P. Nicolete, P. Adriana, V. Aurelia, M. Lavinia, Solid polymer electrolytes based on phosphorus containing polymers for lithium polymer batteries, Eur. Polym. J. 94 (2017) 286–298.
[7] G. Homann, L. Stolz, J. Nair, Poly(ethylene oxide)-based electrolyte for solid-state-lithium-batteries with high voltage positive electrodes: evaluating the role of electrolyte oxidation in rapid cell failure, Sci. Rep. 10 (2020) 4390.
[8] R. Arunkumar, R.S. Babu, M. Usha Rani, S. Kalainathan, Effect of PBMA on PVC-based polymer blend electrolytes, J. *Appl. Polym. Sci* 1*34* (2017) 44939.
[9] N. Farah, H.M. Ng, N. Arshid, C.W. Liew, N.A.A. Latip, K. Ramesh, S. Ramesh, Solid polymer electrolytes based on poly(vinyl alcohol) incorporated with sodium salt and ionic liquid for electrical double layer capacitor, Mater. Sci. Eng., B 251 (2019) 14468.
[10] T.F. Garrison, A. Murawski, R.L. Quirino, Bio-based polymers with potential for biodegradability, Polymers 8 (2016) 1–22.
[11] M.F. Shukur, M.F.Z. Kadir, Hydrogen ion conducting starch-chitosan blend based electrolyte for application in electrochemical devices, Electrochim. Acta 158 (2015) 152–165.
[12] M.S.A. Rani, N.A. Dzulkurnain, A. Ahmad, N.S. Mohamed, Conductivity and dielectric behavior studies of carboxymethyl cellulose from kenaf bast fiber incorporated with ammonium acetate-BMATFSI biopolymer electrolytes, Int. J. Polym. Anal. 20 (2015) 250–260.
[13] V. Moniha, M. Alagar, S. Selvasekarapandian, B. Sundaresan, G. Boopathi, Conductive bio-polymer electrolyte iota-carrageenan with ammonium nitrate for application in electrochemical devices, J. Non-Cryst. Solids 481 (2018) 424–434.
[14] F.H. Muhammad, A. Jamal, T. Winie, Study on factors governing the conductivity performance of acylated chitosan-NaI electrolyte system, Ionics 23 (2017) 3045–3056.
[15] S.N.F. Yusuf, A.D. Azzahari, R. Yahya, S.R. Majid, M.A. Careem, A.K. Arof, From crab shell to solar cell: a gel polymer electrolyte based on N-phthaloylchitosan and its application in dye-sensitized solar cells, RSC Adv. 6 (2016) 27714–27724.
[16] Aziz M. Abdullah, Shujahadeen B. Aziz, Salah R. Saeed, Structural and electric properties of polyvinyl alcohol (PVA): methyl cellulose (MC) based solid polymer blend electrolysis inserted with sodium iodide (NAI) salt, Arab. J. Chem. 14 (2021) 103388.
[17] Amar Ratan, M.H. Buraidah, L.P. Teo, Pramod K. Singh, A.k. Arof, Enhanced photo-current conversion efficiency by incorporation of succinonitrile in N-Phthaloylchitosan based bio-polymer electrolyte for dye sensitized solar cell, Optik 222 (2021) 165467.
[18] K.H.P.S. Abdul, N.A. Sro Aprilia, A.H. Bhat, M. Jawaid, M.T. Paridah, D.A. Rudi, Jatropha biomass as renewable materials for biocomposites and its applications, Renew. Sustain. Energy Rev. 22 (2013) 667–685.
[19] A.S.A. Hazmi, M.M. Aung, L.C. Abdullah, M.Z. Salleh, M.H. Mahmood, Production *Jatropha* oil-based polyol via epoxidation and ring opening, Ind. Crop. Prod. 50 (2013) 563–567.
[20] S. Ibrahim, A. Ahmad, N.S. Mohamed, Characterization of novel castor oil-based polyurethane polymer electrolytes, Polymers 7 (2015) 747–759.
[21] R.A.G. Whba, L. TianKhoon, M.S. Su'ait, M.Y.A. Rahman, A. Ahmad, Influence of binary lithium salts on 49% poly(methyl methacrylate) grafted natural rubber based solid polymer electrolytes, Arab. J. Chem. 13 (1) (2020) 3351–3361.
[22] Nurul Ilham Adam, Hussein Hanibah, Ri Hanum Yahaya Subban, Muhammad Kassim, Nadhratun Naiim Mobarak, Azizan Ahmad, Khairiah Haji Badri, Mohd Sukor Su'ait, Plam -based cationic polyurethane membranes for solid polymer electrolytes application: a physico-chemical characteristics studies of chain-extended cationic polyurethane, Ind. Crop. Prod. 155 (2020) 112757.
[23] L.H. Sim, S.N. Gan, C.H. Chan, R. Yahya, ATR-FTIR studies on ion interaction of lithium perchlorate in polyacrylate/poly(ethylene oxide) blends, Spectrochim. Acta Mol. Biomol. Spectrosc. 76 (2010) 287–292.
[24] Y.S. Lim, A.J. Hyun, H. Hwang, Fabrication of PEO-PMMA-LiClO4-based solid polymer electrolytes containing silica aerogel particles for all-solid-state lithium batteries, Energies 11 (2018) 2559.
[25] D. Saikia, Y.H. Chen, Y.C. Pan, J. Fang, L.D. Tsai, G.T.K. Fey, H.M. Kao, A new highly conductive organic-inorganic solid polymer electrolyte based on a di-ureasil matrix doped with lithium perchlorate, J. Mater. Chem. 21 (2011) 10542.
[26] P. Santhosh, A. Gopalan, T. Vasudevan, K.P. Lee, Evaluation of a cross-linked polyurethane acrylate as polymer electrolyte for lithium batteries, Mater. Res. Bull. 41 (6) (2006) 1023–1037.
[27] Y.T. Chen, Y.C. Chuang, J.H. Su, H.C. Yu, Y.W. Chen-Yang, High discharge capacity solid composite polymer electrolyte lithium battery, J. Power Sources 196 (2011) 2802–2809.
[28] L. Feng, Z. Xing, L.I. Hong, L.A.I. Xue, Z. Fu, Synthesis and properties of UV curable polyurethane acrylates based on two different hydroxyethyl acrylates, J. Cent. S. Univ. 19 (2012) 911–917.
[29] E. Nieto, New Polyurethanes from Vegetable Oil-Based Polyols, 2011.
[30] C.S. Wong, K.H. Badri, N. Ataollahi, K.P. Law, M.S. Su'ait, N.I. Hassan, Synthesis of new bio-based solid polymer electrolyte effect of NCO/OH ratio on their chemical, thermal properties and ionic conductivity, Int. J. Civ. Mech. Eng. 8 (11) (2014) 1234–1250.
[31] C. Muthuvinayagam, C. Gopinathan, Characterization of proton conducting polymer blend electrolytes based on PVdF-PVA, Polymer 68 (2015) 122–130.
[32] Z. Fang, M. Zhou, J. Zhong, Y. Qi, L. Li, Q. Dong, Preparation and properties of novel ultraviolet-cured waterborne polyurethanes, High Perform. Polym. 25 (2013) 668–676.
[33] M. Ulaganathan, R. Nithya, S. Rajendran, Surface analysis studies on polymer electrolyte membranes using scanning electron microscope and atomic force microscope, Scanning Electron. Microsc. (2012) 671–694.
[34] M. Imperiyka, A. Ahmad, S.A. Hanifah, M.Y.A. Rahman, Preparation and characterization of polymer electrolyte of with ethylene carbonate, Int. J. Polym. Sci. (2014) 1–7.
[35] P.K. Singh, B. Bhattacharya, R.K. Nagarale, K.W. Kim, H. W. Synthesis Rhee, Characterization and application of biopolymer-ionic composite membranes, Synth. Met. 160 (2010) 139–142.
[36] F.N. Jumaah, N.N. Mobarak, A. Ahmad, M.A. Ghani, M.Y.A. Rahman, Derivative of iota-carrageenan as solid polymer electrolyte, Ionics 21 (2015) 1311–1320.
[37] M.S. Su'ait, A. Ahmad, K.H. Badri, N.S. Mohamed, M.Y.A. Rahman, C.L.A. Ricardo, P. Scardi, The potential of polyurethane bio-based solid polymer electrolyte for photoelectrochemical cell application, Int. J. Hydrogen Energy 39 (6) (2014) 3005–3017.
[38] A.K. Arof, I.M. Noor, M.H. Buraidah, T.M.W.J. Bandara, M.A. Careem, I. Albinsson, B.E. Mellander, Polyacrylonitrile gel polymer electrolyte based dye sensitized solar cells for a prototype solar panel, Electrochim. Acta 251 (2017) 223–234.
[39] W.H. Hou, C.Y. Chen, C.C. Wang, Y.H. Huang, The effect of different lithium salts on conductivity of comb-like polymer electrolyte with chelating functional group, Electrochim. Acta 48 (2003) 679–690.
[40] C.S. Ramya, S. Selvasekarapandian, G. Hirankumar, T. Savitha, P.C. Angelo, Investigation on dielectric relaxations of PVP-NH4SCN polymer electrolyte, J. Non-Cryst. Solids 354 (2008) 1494–1502.
[41] D.K. Pradhan, R.N.P. Choudhary, B.K. Samantaray, Studies of dielectric relaxation and AC conductivity behavior of plasticized polymer nanocomposite electrolytes, Int. J. Electrochem. Sci. 3 (2008) 597–608.
[42] A.S. Samsudin, H.M. Lai, M.I.N. Isa, Biopolymer materials based carboxymethyl cellulose as a proton conducting biopolymer electrolyte for application in rechargeable proton battery, Electrochim. Acta 129 (2014) 1–13.
[43] A.S.A. Khiar, R. Puteh, A.K. Arof, Conductivity studies of a chitosan-based polymer electrolyte, Phys. B Condens. Matter 373 (2006) 23–27.
[44] M. Saiful, A. Rani, S. Rudhziah, A. Ahmad, N.S. Mohamed, Biopolymer Electrolyte Based on Derivatives of Cellulose from Kenaf Bast Fiber, 2014, pp. 2371–2385.
[45] J. Zhang, X. Huang, H. Wei, J. Fu, Y. Huang, X. Tang, Enhanced electrochemical properties of polyethylene oxide-based composite solid polymer electrolytes with porous inorganic-organic hybrid polyphosphazene nanotubes as fillers, J. Solid State Electrochem. 16 (2012) 101–107.
[46] S. Monisha, T. Mathavan, S. Selvasekarapandian, A.M.F. Benial, M.P. Latha, Preparation and characterization of cellulose acetate and lithium nitrate for advanced electrochemical devices, Ionics (2016) 1–10.